ELSEVIER

Thermochimica Acta 258 (1995) 1–14

thermochimica acta

Calorespirometric analysis of plant tissue metabolism using calorimetry and pressure measurement

A.J. Fontana [a], K.L. Hilt [a], D. Paige [b], L.D. Hansen [c], R.S. Criddle [a,*]

[a] *Section of Molecular and Cellular Biology, University of California, Davis, CA 95616, USA*
[b] *Agronomy and Range Science, University of California, Davis, CA 95616, USA*
[c] *Department of Chemistry and Biochemistry, Brigham Young University, Provo, UT 84602, USA*

Received 9 November 1994; accepted 2 January 1995

Abstract

Methods and equipment are described for simultaneous measurements of heat flow rates, CO_2 evolution rates, O_2 use rates and sample volumes for three samples in a differential heat conduction calorimeter. Isothermal measurements of metabolic heat rates were conducted in 1 ml sealed ampoules connected to pressure sensors. Pressure measurements in the presence and absence of a CO_2 trapping solution allow determination of the gas flux rates. The decrease in the partial pressure of O_2 within the sealed ampoule under trapping conditions measures O_2 consumption by the tissue. The CO_2 rates are determined by two methods. Absorption of CO_2 produces heat at a rate proportional to the rate of CO_2 production. Also, the difference between the rate of change of pressure with and without trapping solution yields the CO_2 production rate by the tissue. Measuring gas flux by pressure change requires knowledge of headspace volume. Two methods of headspace volume determination are discussed. The first involves the introduction of a mass of known volume into the ampoule during pressure change measurements and the second involves recording the pressure increase upon addition of a known volume of gas into the ampoule. The methods described here are useful for studies of metabolic efficiency in biomass production and examination of responses of cell metabolism to changes in environmental or physiological conditions.

Keywords: Calorespirometry; Metabolic heat; Plant metabolism; Respiration

* Corresponding author.

SSDI 0040-6031(95)02251-1

1. Introduction

This report describes methods for simultaneous heat flow rate, O_2 use and CO_2 evolution rate measurements in 1 ml calorimeter vessels. Measurements of oxygen uptake rate by gas trapping and pressure change methods for both O_2 and CO_2 date back to instruments described by Barcroft and Haldane [1] and Warburg [2]. The use of simultaneous measurements of the rates of heat production, CO_2 production, and O_2 uptake for determination of plant growth rates is described in earlier work by Criddle, Hansen and co-workers [3–5].

Measurement of the rate of heat production simultaneous with CO_2 production or O_2 use by living tissues provides useful information on metabolic pathways and efficiency differences in biological tissues [6–10]. The methods of plant calorespirometry described earlier by Criddle et al. [11,12] have provided major insight into plant energy metabolism, while showing that enhanced capabilities are required for accurate, simultaneous determination of all three respiratory rates on small (< 250 mg) samples.

The earlier publication [12] described means for O_2 and CO_2 rate measurements consisting of one pressure sensor connected to two calorimetric ampoules. Respiring tissue was placed in one ampoule and the trapping solution in the other. With this arrangement, the metabolic heat rate was measured directly in one ampoule and the rate of CO_2 production in the other. This system functioned adequately with large (> 50 ml) calorimeter vessels, but not with small vessels. Measurement times were long, limiting the number of samples that could be examined. The new design of the pressure measuring system described here allows gas flux measurements simultaneously in the three 1 ml sample ampoules of a Hart Scientific Model 7707 calorimeter. In addition, special ampoules were constructed with a ring welded inside to hold a metal vial of CO_2 trapping solution in better thermal contact than in the glass vials previously described.

Further improvements were made in connecting the ampoules to the pressure sensors. Previously, PEEK (Upchurch Scientific) tubing was used. The thick wall of this tubing acts as a heat sink, creating problems with non-ambient temperature heat rate measurements. The current system uses thin-wall, fused-silica capillary tubing to connect the ampoules to the pressure sensors. In addition, the reference ampoule is connected to the reference side of all three differential pressure sensors. The differential arrangement allows pressure measurements while scanning the temperature. This arrangement is required for temperature scanning experiments because the absolute pressure change is large and can damage the narrow-range sensors required for optimal sensitivity. The pressure changes in sample and reference ampoules during scanning are largely canceled in this differential arrangement. Further improvements include controlling the temperature of the pressure sensors to improve stability, and addition of a pressure reset port to allow resetting of the pressure to ambient after the ampoule has been closed and to permit determination of the headspace volume in the sample ampoule. The improved system allows simultaneous measurements of heat flow rate, CO_2 evolution rate, O_2 use rate and sample volume on three samples.

2. Materials and methods

A Hart Scientific Model 7707 differential scanning calorimeter with four removable, cylindrical, 1 ml Hastelloy ampoules with screw lids was used in this work. One of the ampoules served as a reference, allowing simultaneous measurements of heat flow rates and pressure changes on three samples. Two different types of ampoules were used, the standard ampoule supplied with the calorimeter into which a 40 µl glass vial filled with either water or sodium hydroxide solution was placed, or ampoules with rings welded inside to hold a 40 µl Hastelloy vial. The lids of the ampoules were connected to the pressure sensors with 30 cm length and 0.32 mm i.d. fused-silica capillary tubing (J&W Scientific) sealed into holes in the lids with polyamine–polyamide–epoxy resin. The capillary was connected to the pressure sensor with a 1/16 in. Swagelok® connector with either Teflon or VG2 Vespel®/Graphite ferrules (Alltech).

Three SenSym SX01 (SenSym) pressure sensors are connected as shown in Fig. 1. The SenSym SX01 is a miniaturized, full bridge, strain gauge differential pressure sensor with a full scale range of 6.89 kPa. The sensors are powered with a 6.9 V power supply consisting of a 24 V center-tapped transformer, a full-wave rectifier, an LM7812 preregulator, and an LM399 thermally stabilized reference source. The output voltage of the pressure sensors changes linearly with applied pressure.

Calibration of the pressure sensors employed a 23 cm, two revolution, mirror scale precision pressure gauge (Wallace and Tiernan, Belleville, NJ) reading in inches of water at 20°C. A 5 ml gas tight syringe (Hamilton) connected to the sensor and gauge through the pressure reset port (Fig. 2) was used to calibrate the sensors at pressures above ambient. The sensors were calibrated at sub-ambient pressures by connecting to the reference side of the sensors. Calibrations were done in 2 in. increments from 0 to 30 in. of H_2O and gauge values were converted to atmospheres and bar by 1 atm = 407.515 in. of water at 20°C = 1.01325 bar. Table 1 gives the results of linear regression of the calibration data for the pressure sensors.

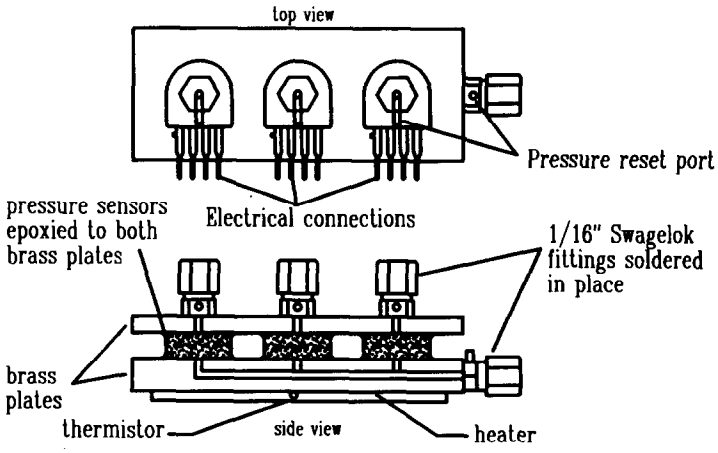

Fig. 1. Schematic drawing of the three pressure sensor system.

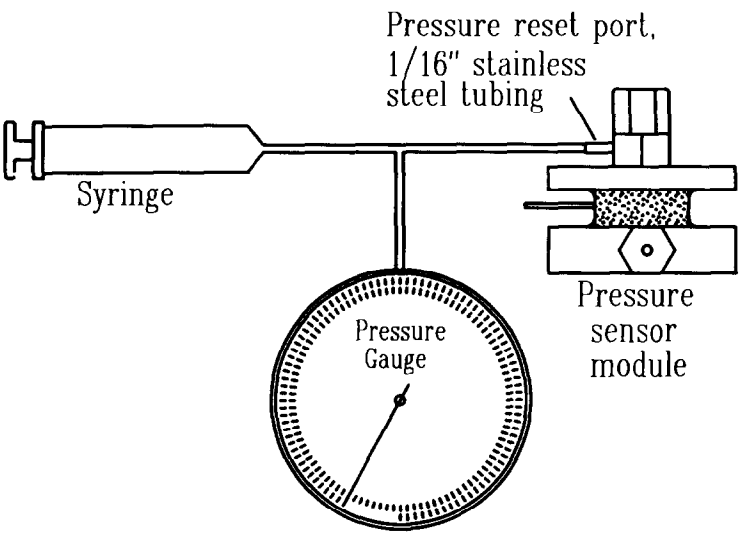

Fig. 2. Schematic drawing of connections to pressure sensor during calibration.

Table 1
Results of pressure sensor calibration

Sensor	Slope in bar V^{-1}	Intercept in bar	R^2 [a]
1	0.2153 ± 0.0003	0.8883 ± 0.0004	0.99994
2	0.1865 ± 0.0002	0.9489 ± 0.0003	0.99996
3	0.2056 ± 0.0002	0.9901 ± 0.0003	0.99997

[a] $n = 30$.

Accurate determination of the total volume of the ampoule and the pressure detection system is essential for the calculation of absolute gas exchange rates. The volume of the system includes the volumes inside the ampoule, glass capillary tubing, Swagelok® connector, pressure reset port, hole in brass plate, and the pressure sensor. During actual measurements the reset port is closed with a flat silicone rubber cap. Measurement of the total empty volume was done with the apparatus shown in Fig. 3. The pipette and tubing were initially filled with water except for a small amount of air in the end of the tubing connected to the pressure reset port. The initial level of water in the pipette and the pressure (voltage) are recorded after the tubing is connected. Using the syringe on top of the pipette, pressure above the water is increased until the water is exactly even with the end of the pressure reset port. The new level of water in the pipette and the new pressure voltage are recorded. The volume of the system is calculated using Boyle's law:

$$P_1 V_1 = P_2 V_{\text{system}} \tag{1}$$

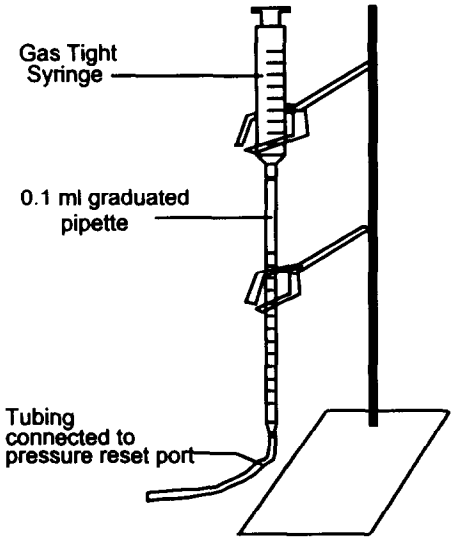

Fig. 3. Schematic drawing of the apparatus used to determine the volume of the headspace and tissue within the ampoule.

where $P_{1,2}$ are the measured pressures, V_{system} is the total empty volume of the ampoule system, and V_1 is the total volume of the ampoule system plus the small volume of air initially in the tubing. The volume of air initially in the tubing is the volume difference of the pipette readings ΔV.

$$V_1 = V_{system} + \Delta V \tag{2}$$

Combining Eqs. (1) and (2) gives

$$V_{system} = P_1 \Delta V/(P_2 - P_1) \tag{3}$$

Table 2 lists the results of volume determinations of the ampoule systems.

During respiration measurements, it is essential to know the volume of gas within the ampoule system with the sample present. Two methods of determining the headspace volume with a sample in the ampoule have been tested. The first method uses the same equipment and method used to determine the volume of the empty ampoule system, Fig. 3. At the beginning or end of a calorespirometric measurement, the apparatus is connected to the pressure reset port and the system volume is measured with the sample in place. The second method involves introduction of an unreactive mass of known volume into the ampoule together with the tissue under CO_2 trapping conditions. Assuming a constant O_2 uptake rate by the tissue, and that all CO_2 is absorbed, the smaller headspace results in a greater change in pressure with time when the mass is present than when it is not. Under conditions of no added mass

$$(dp/dt)_1 = RT(dn/dt)/V_1 \tag{4}$$

Table 2
Determination of the volume in ml of the ampoules and connected system

Ampoule	Volume	Standard deviation of the mean[a]
1	1.277	±0.002
2	1.262	±0.002
3	1.259	±0.003
1 + vial	1.235	±0.002
2 + vial	1.224	±0.003
3 + vial	1.199	±0.005
4 reference	1.543	±0.005

[a] $n = 6$.

and under conditions of additional mass

$$(dp/dt)_2 = RT(dn/dt)/V_2 \tag{5}$$

where R is the gas constant and T is the absolute temperature. The ratio of Eqs. (4) and (5) simplifies to

$$(dp/dt)_1/(dp/dt)_2 = V_2/V_1 \tag{6}$$

where $V_1 = V_{system} - V_{sample}$ and $V_2 = V_{system} - V_{sample} - V_{mass}$. Since the volume of the system and the mass are known, the volume of the headspace with tissue present is

$$V_1 = V_{mass}[1 - (dp/dt)_1/(dp/dt)_2]^{-1} \tag{7}$$

A piece of 1/8 in. copper wire was used as the additional mass. The volume of copper was calculated from the mass and the density, 8.92 g ml^{-1} [13].

As an independent check of the pressure and volume calibrations, and as an example of an application to determination of volume changes during scanning calorimetry, the pressure change associated with the volume change during melting of a known amount of ice was measured. The density of ice is 0.917 g ml^{-1} and that of liquid water is 0.99987 g ml^{-1} at 0°C [13]. The change in state from ice to water results in a net increase in headspace volume and, because the ampoule is a closed system, a pressure decrease proportional to the volume change of water is observed.

Approximately 25, 50, and 100 µl volumes of water were pipetted into the three ampoules and accurately weighed. The exact volume of water was determined from the mass and the density of water at the laboratory temperature. The ampoules were then placed in the calorimeter, rapidly brought to −20°C, and held at this temperature for 1 h. The ampoules were then scanned up to 20°C at a rate of 6 K h^{-1}.

3. Results

The results of the two methods for measurements of headspace volume with samples of redwood meristem tissue in each ampoule are shown in Table 3. The two methods

Table 3
Determination of headspace volume in ml with redwood meristem tissue

Ampoule	Method 1[a]	Method 2[b]
1	1.079 ± 0.001	1.082 ± 0.001
2	1.026 ± 0.002	1.027 ± 0.001
3	1.001 ± 0.003	0.998 ± 0.001

[a] Method using apparatus shown in Fig. 3.
[b] Method using added mass of known volume.

agree and provide two distinct measures of the headspace volume. The error in method 1 is the standard deviation of the mean of three measurements. The error in method 2 is calculated from the error in the linear regression of pressure with time.

Fig. 4 shows the measured pressure changes associated with the melting of ice. The baselines slope upward because the pressure increases with increasing temperature. At 0°C the ice begins to melt and there is a pressure decrease in the ampoule. By the time the calorimeter block temperature reaches 1.5°C, all of the ice has melted and the pressure increase is again linear. The temperature in the ampoule must remain at 0°C until all ice has melted, then the temperature will increase rapidly to near the block temperature. The rise in pressure occurring after the ice melts is caused by the increase in water vapor pressure as the ampoule temperature rises to the block temperature. The

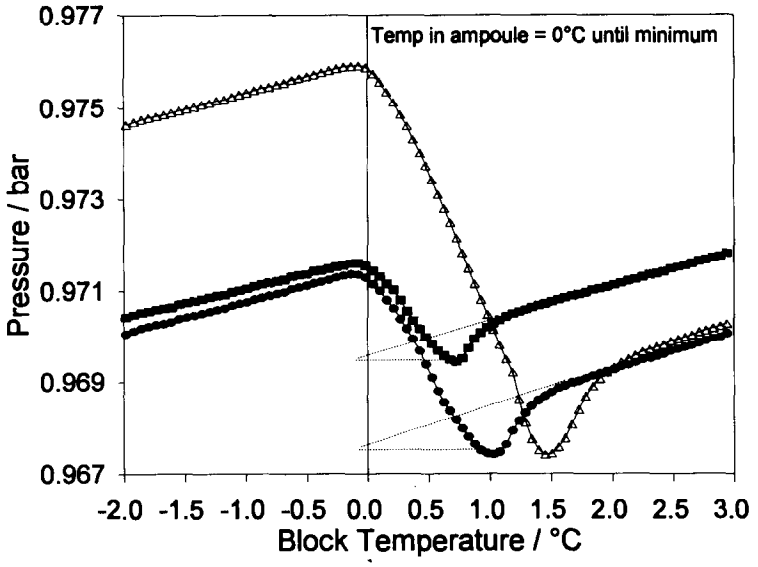

Fig. 4. Pressure curves due to the volume change of melting of ice to (■) 25, (●) 49, and (△) 96 μl of water in the sealed ampoules.

dashed lines in the figure show that, after the vapor pressure over the liquid water has stabilized, the extrapolated value at 0°C yields the same pressure value as that measured from the minimum for ice melting.

Table 4 compares measured volume changes with the changes calculated from the masses of water and known differences between the densities of ice and water. The data show agreement between the calculated and the measured volume changes. This experiment demonstrates that the pressure sensor system can be used to measure volume changes as small as 3 μl.

Fig. 5 illustrates metabolic heat rate data obtained at 25°C with redwood tissue. The curves of heat flow rate show an initial period of changing power output as the calorimeter approaches thermal equilibrium, followed by a steady-state rate indicative of the metabolic heat rate of the tissue. The first part of the isothermal experiment measured the metabolic heat rate with 40 μl of water in the vial. In the second part, 40 μl of 0.4 M NaOH was filled in place of the water, the ampoule was resealed and replaced in the calorimeter and the heat flow rate was again determined. In the third part of the experiment, the NaOH solution was replaced with fresh solution, a block of copper was inserted, and the heat flow rate was measured again. The fourth part of the experiment repeated the first part to ensure that the metabolism had not changed significantly during the experiment.

The pressure data collected in the experiment are shown in Fig. 6. Accurate pressure measurements can be made much earlier than required for heat flow rate measurements, as the small temperature changes of thermal equilibration have a negligible effect on pressure. The slopes dp/dt of the curves in the first and last parts of the figure are proportional to the difference between the rates of CO_2 production and O_2 depletion. With the NaOH solution present, all of the CO_2 produced is absorbed and the slopes of the curves in the second and third parts of the experiment are proportional

Table 4
Results of measurements of volumes change for melting of ice

		Ampoule 1	Ampoule 2	Ampoule 3
Mass of H_2O	mg	25.17	49.35	96.06
Volume of ice	μl	27.34	53.82	104.75
Volume of H_2O	μl	25.17	49.36	96.07
Headspace gas pressure				
0°C ice	bar	0.9718	0.9710	0.9759
0°C H_2O	bar	0.9697	0.9670	0.9676
Headspace volume[a]				
0°C ice	μl	1197	1160	1107
0°C H_2O	μl	1199	1165	1116
Volume change				
Calculated	μl	2.17	4.46	8.68
Measured[b]	μl	2.6	4.7	9.4
Difference	%	+20	+5	+8

[a] Measured with apparatus shown in Fig. 3, i.e. method 1.
[b] See Eq. (3).

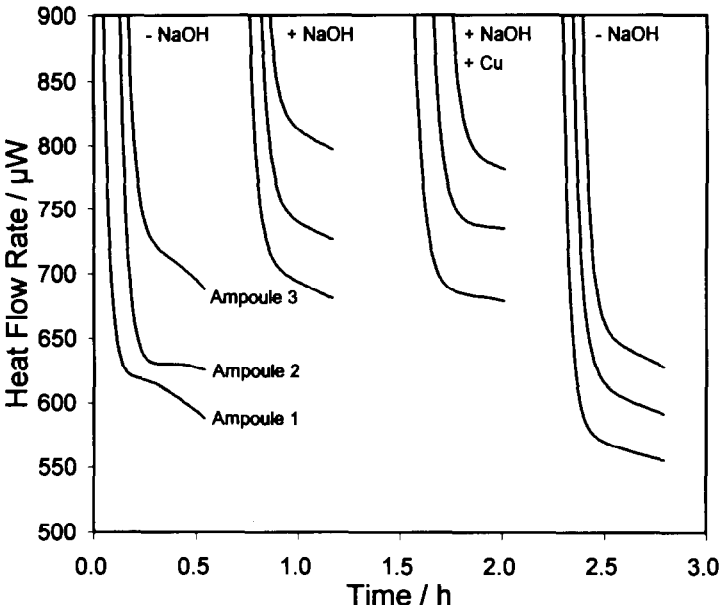

Fig. 5. Metabolic heat rates of redwood tissue with and without NaOH trapping and with a copper mass added to the ampoule.

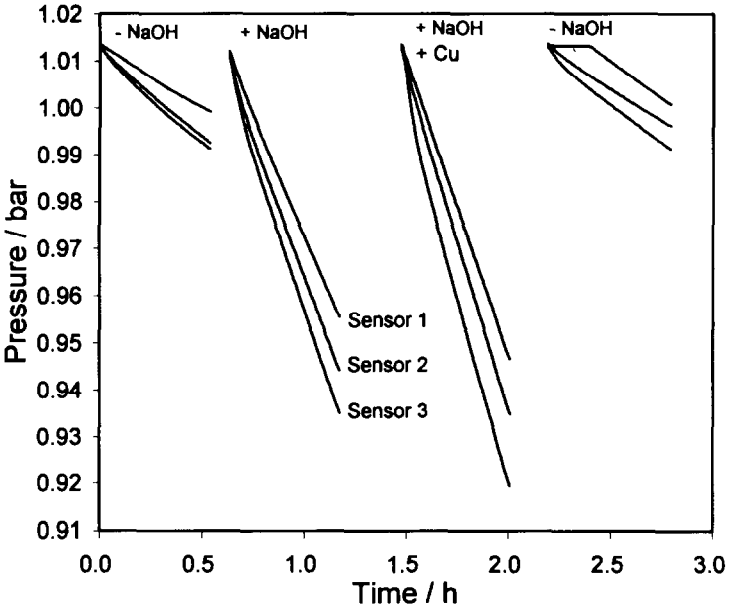

Fig. 6. Pressure sensor results for redwood tissue with and without NaOH trapping and with a copper mass added to the ampoule.

to the rate of O_2 use. The slopes of the third set of curves, with copper added to the ampoule, are steeper than the second set because the headspace volume is smaller, and therefore, the change in pressure is greater for the same O_2 use rate. The sign of the slope $(dp/dt)_1$ indicates additional information. If $(dp/dt)_1$ is positive, then $R_{CO_2} > R_{O_2}$ and the gas exchange quotient is >1, whereas if $(dp/dt)_1$ is negative then $R_{CO_2} < R_{O_2}$ and the gas exchange quotient is <1.

Table 5 summarizes the information obtained from the experiment shown in Figs. 5 and 6. The data enables two independent determinations of CO_2 rate. In one, CO_2 rate is obtained from the difference in heat flow rates, and in the other, CO_2 rate is determined from the difference in dp/dt with and without the NaOH solution present. From Fig. 5, the metabolic heat rate of the tissue is the average of $\dot{q}_1$ and $\dot{q}_4$. The symbol $\dot{q}$ is used here for heat flow rate to be consistent with use in other plant studies and to avoid confusion that may arise in the plant field from using Φ for this quantity. The heat flow rate under trapping conditions $(\dot{q}_2 + \dot{q}_3)/2$, is the metabolic heat rate of the tissue plus the heat flow rate from neutralization of NaOH by CO_2. Thus, the heat flow rate from reaction of CO_2 is

$$\Delta\dot{q} = 0.5(\dot{q}_2 + \dot{q}_3 - \dot{q}_1 - \dot{q}_4) \tag{8}$$

and the CO_2 rate is

$$R_{CO_2} = \Delta\dot{q}/108.5 \tag{9}$$

where the constant 108.5 kJ mol^{-1} is the enthalpy of reaction of 0.4 M NaOH with CO_2(g) at 25°C [14]. The slopes $(dp/dt)_1$ and $(dp/dt)_4$ in Fig. 6 are proportional to the rate of CO_2 production minus the rate of O_2 use. Under trapping conditions, all of the CO_2 produced is absorbed by the NaOH solution, and the slope $(dp/dt)_2$ is the O_2 use rate. The difference between $[(dp/dt)_1 + (dp/dt)_4]/2$ and $(dp/dt)_2$ is the CO_2 rate as

Table 5
Results of measurements on redwood meristem tissue

	Units	Ampoule Number		
		1	2	3
$(\dot{q}_1 + \dot{q}_4)/2$	μW mg (DW)$^{-1}$	7.93 ± 0.01	6.99 ± 0.01	7.54 ± 0.01
$(\dot{q}_2 + \dot{q}_3)/2$	μW mg (DW)$^{-1}$	9.39 ± 0.01	8.40 ± 0.01	9.07 ± 0.01
$\Delta\dot{q}$	μW mg (DW)$^{-1}$	1.46 ± 0.01	1.41 ± 0.01	1.53 ± 0.01
V_{system}	ml	1.039 ± 0.002	0.986 ± 0.002	0.961 ± 0.002
Sample dry weight (DW)	mg	72.94 ± 0.05	87.27 ± 0.05	87.62 ± 0.05
$0.5((dp/dt)_1 + (dp/dt)_4)V_{system}/RT$	pmol s^{-1} mg(DW)$^{-1}$	4.30 ± 0.02	4.36 ± 0.02	4.28 ± 0.02
$(dp/dt)_2 V_{system}/RT, R_{O_2}$	pmol s^{-1} mg(DW)$^{-1}$	17.90 ± 0.05	17.38 ± 0.05	18.67 ± 0.05
R_{CO_2} [a]	pmol s^{-1} mg(DW)$^{-1}$	13.46 ± 0.04	12.99 ± 0.04	14.10 ± 0.04
R_{CO_2} [b]	pmol s^{-1} mg(DW)$^{-1}$	13.60 ± 0.05	13.02 ± 0.05	14.39 ± 0.05

[a] Using Eq. (9).
[b] Using Eq. (11).

shown in Eqs. (10) and (11).

$$R_{CO_2} = (R_{CO_2} - R_{O_2}) - (-R_{O_2}) \tag{10}$$

$$R_{CO_2} = [0.5((dp/dt)_1 + (dp/dt)_4) - (dp/dt)_2]\, V_{system}/RT \tag{11}$$

The two methods provide an internal check on the experimental results. The data show that, within the uncertainties, both methods give the same CO_2 production rate for the redwood tissue.

It is essential to supply excess NaOH in the trapping solution and to have adequate surface area of the NaOH solution so that rates of CO_2 absorption do not become limiting. To check the adequacy of the trap, an experiment was done with two NaOH vials instead of one and with a larger tissue sample than normally used. Fig. 7 shows the results of the experiment. Initially the two vials were filled with water. After the heat flow rate had reached an approximately steady state, the ampoule was opened and the water in one of the vials was replaced with 40 µl of NaOH. The ampoule was resealed and again the heat flow rate was allowed to reach steady state. The ampoule was opened for a second time to fill the second vial with 40 µl of trapping solution. A heat flow rate of 848 ± 2 µW was obtained with one trap and 850 ± 2 µW with two traps. The rate of change of pressure was 0.146 ± 0.005 with one trap and 0.143 ± 0.005 bar h^{-1} with two traps. This experiment clearly shows that one vial containing 40 µl of 0.4 M NaOH is sufficient even at large total metabolic rates.

All the methods for measuring CO_2 rate are subject to error if the sample or the water present absorbs a significant amount of CO_2 during any part of the experiment [15]. For example, in the experiment described in Figs. 6 and 7, as the partial pressure of CO_2

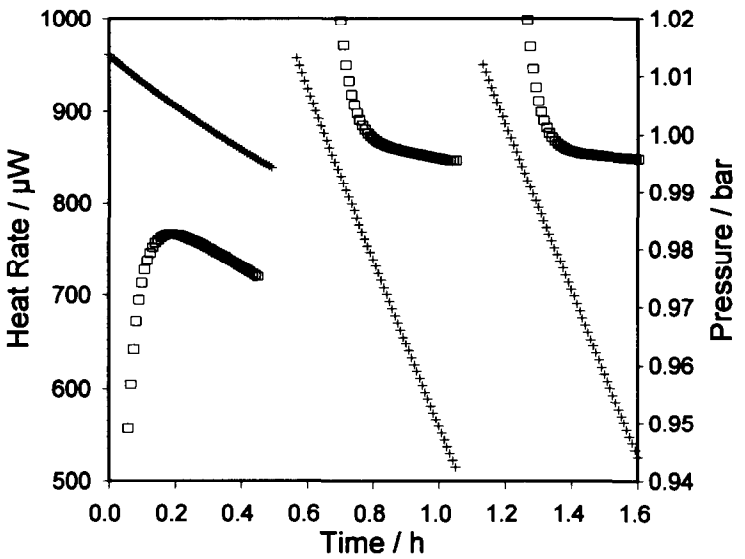

Fig. 7. Metabolic heat rate (□) and pressure (+) measurements on redwood meristem tissue using no, one and two traps.

increases due to metabolism within the ampoule, more CO_2 will dissolve in the water. CO_2 dissolved in the water will not be detected by the pressure sensor or absorbed by the trapping solution. Both cases will result in an erroneously low CO_2 rate. Calculations show that the concentration of CO_2 dissolved in the water in this experiment is not significant, i.e. <0.01%, but the presence of CO_2-reactive material such as Hoagland's solution could lead to sizable error and must be avoided.

4. Discussion

This study demonstrates the development and use of methods and equipment linking respirometry and calorimetry for determining important metabolic parameters in biological tissues. The methods are useful for studies of efficiency of production of biomass, investigation of tissues subjected to changes in biological control, and examination of alterations of cell metabolism in response to a wide range of changed environmental or physiological conditions. The growth rates and biomass production rates of plants depend upon the metabolic rate and how effectively plants use metabolic energy. Both are measurable by calorespirometric techniques. By use of thermodynamic models describing the relationship between plant growth and respiration, the genetic growth potential of a plant can be determined (Hansen et al. [4, 5]).

From experimental results such as those in Table 5, additional important plant metabolic information can be obtained. For example, the gas exchange quotient, i.e. the mole ratio of the rate of production of CO_2 to the rate of consumption of O_2 in growing tissue, is related to the oxidation state of carbon in the substrate being consumed (γ_p), the oxidation state of carbon in the biomass being produced (γ_B), and to the efficiency of carbon use (ε) as shown in Eq. (12).

$$R_{CO_2}/R_{O_2} = [(1 - \gamma_p/4) + \varepsilon(\gamma_B - \gamma_p)/4(1 - \varepsilon)]^{-1} \tag{12}$$

The ratio measured for the redwood tissue used in these studies is 0.76 ± 0.01, a value appropriate for this tissue in early January when stored lipids and proteins are being metabolized. The value of the ratio $\dot{q}/R_{O_2}$, $-403\,\mathrm{kJ\,mol^{-1}}$, is less than the constant in Thornton's rule of $-455\,\mathrm{kJ\,mol^{-1}}$ O_2 [16, 17] often used in indirect calorimetry, because this ratio is also a function of γ_p, γ_B, and ε as shown in Eq. (13).

$$\dot{q}/R_{O_2} = [(1 - \gamma_p/4)(455) + \Delta H_B\varepsilon/(\varepsilon - 1)]/[(1 - \gamma_p/4) + \varepsilon(\gamma_B - \gamma_p)/4(1 - \varepsilon)] \tag{13}$$

where ΔH_B is the enthalpy change for conversion of substrate to biomass.

The ratio of heat flow rate to CO_2 rate had values of 536 and $531\,\mathrm{kJ\,mol^{-1}}$ for the trapping and the pressure slope method, respectively. The two methods agree and are an internal check that the measurements are correct. The heat flow rate per CO_2 rate is also a function of γ_p, ε, and ΔH_B as shown in Eq. (14).

$$\dot{q}/R_{CO_2} = (1 - \gamma_p/4)(455) + (\varepsilon/\varepsilon - 1)\Delta H_B \tag{14}$$

These equations, together with the equation for specific growth rate

$$R_{SG} = [-\dot{q} + 455(1 - \gamma_p/4)R_{CO_2}]/\Delta H_B \tag{15}$$

can be used to predict plant growth rates and to understand why growth rates differ among individuals within a species [18] and among related species [19].

The techniques described here can be applied to tissue sections, microbial and eukaryotic cells and whole organisms that can be grown in air or modified gas mixtures. Measurements can be made on viable tissues under near-physiological conditions. The method should provide an important additional tool for the study of metabolism. Other applications of the method include kinetic analysis of chemical reactions in which heat flow rates and changes in gas concentrations can be simultaneously monitored to investigate reaction mechanisms, e.g. oxidation rates and stoichiometry for oxidative degradation of food products [20] and pharmaceuticals [21, 22]. The differential design of the pressure sensing system allows determination of volume changes for reactions occurring during scanning experiments, as shown by experiments in which ice was melted.

References

[1] J. Barcroft and J.S. Haldane, J. Physiol., 28 (1902) 232–240.
[2] O. Warburg, Über den Stoffwechsel der Tumoren, Springer, Berlin, 1926.
[3] R.S. Criddle, R.W. Breidenbach and L.D. Hansen, Plant calorimetry: how to quantitatively compare apples and oranges, Thermochim. Acta, 193 (1991) 67–90.
[4] L.D. Hansen, M.S. Hopkin, D.R. Rank, T.S. Anekonda, R.W. Breidenbach and R.S.Criddle, The relation between plant growth and respiration: A thermodynamic model, Planta, 194 (1994) 77–85.
[5] L.D. Hansen, M.S. Hopkin, D.K. Taylor, T.S. Anekonda, D.R. Rank, R.W. Breidenbach and R.S. Criddle, Plant calorimetry, II: Modeling the difference between apples and oranges, Thermochim. Acta, 250 (1995) 215–232.
[6] E. Gnaiger, J.M. Shick and J. Widdows, Metabolic microcalorimetry and respirometry of aquatic animals, in C.R. Bridges and P.J. Butler (Eds.), Techniques in Comparative Respiratory Physiology. An Experimental Approach, Society for Experimental Biology Seminar Series, Cambridge University Press, 1989, pp. 113–135.
[7] E. Gnaiger, Heat dissipation and energetic efficiency in animal anoxibiosis: economy contra power, J. Exp. Zool., 228 (1983) 471–490.
[8] E. Gnaiger and R.B. Kemp, Anaerobic metabolism in aerobic mammalian cells: information from the ratio of calorimetric heat flux and respirometric oxygen flux, Biochim. Biophys. Acta, 1016 (1990) 328–332.
[9] U. von Stockar and B. Birou, The heat generated by yeast cultures with a mixed metabolism in the transition between respiration and fermentation, Biotechnol. Bioeng., 34 (1989) 86–101.
[10] C. Eftimiadi and G. Rialdi, Increased heat production proportional to oxygen consumption in human neutrophils activated with phorbol-12-myristate-13-acetate, Cell Biophys., 4 (1982) 231–244.
[11] R.S. Criddle, R.W. Breidenbach, D.R. Rank, M.S. Hopkin and L.D. Hansen, Simultaneous calorimetric and respirometric measurements on plant tissues, Thermochim. Acta, 172 (1990) 213–221.
[12] R.S. Criddle, A.J. Fontana, D.R. Rank, D. Paige, L.D. Hansen and R.W. Breidenbach, Simultaneous measurement of metabolic heat rate, CO_2 production, and O_2 consumption by microcalorimetry, Anal. Biochem., 194 (1991) 413–417.
[13] R.C. Weast (Ed.), CRC Handbook of Chemistry and Physics, Chemical Rubber Publishing Co., Cleveland, Ohio, 1977.
[14] D.D. Wagman, W.H. Evans, V.B. Parker, R.H. Schumm, I. Halow, S.M. Bailey, K.L. Churney and R.L. Nuttall, The NBS tables of chemical thermodynamic properties. Selected values for inorganic and C_1 and C_2 organic substances in SI units, J. Phys. Chem. Ref. Data, Vol. II (Suppl. 2) (1982).
[15] T. Naganawa and K. Kyuma, Reversible CO_2 sorption by soils: an error factor in the measurement of soil respiration, Soil Sci. Plant Nutr., 38 (1992) 179–182.

[16] L.E. Erickson, Energy requirements in biological systems, in A.M. James (Ed.), Thermal and Energetic Studies of Cellular Biological Systems, IOP Publishing, Bristol, UK 1987, pp. 14–33.
[17] W.M. Thornton, The relation of oxygen to the heat of combustion of organic compounds, Philos. Mag., Sixth Ser., 33 (1917) 196–223.
[18] T.S. Anekonda, R.S. Criddle, W.J. Libby, R.W. Breidenbach and L.D. Hansen, Respiration rates predict differences in growth of coast redwood, Plant, Cell Environ., 17 (1994) 197–203.
[19] R.S. Criddle, T.S. Anekonda, R.W. Breidenbach and L.D. Hansen, Site-fitness and growth-rate selection of *Eucalyptus* for biomass production, Thermochim. Acta, 251 (1995) 335–349.
[20] A.J. Fontana, L. Howard, R.S. Criddle, L.D. Hansen and E. Wilhelmsen, Kinetics of deterioration of pineapple concentrate, J. Food Sci., 58 (1993) 1411–1417.
[21] L.D. Hansen, E.A. Lewis, D.J. Eatough, R.G. Bergstrom and D. Degraft-Johnson, Kinetics of drug decomposition by heat conduction calorimetry, Pharm. Res., 6 (1989) 20–27.
[22] L.D. Hansen, D.J. Eatough, E.A. Lewis, R.G. Bergstrom, D. Degraft-Johnson and K. Cassidy-Thompson, Shelf-life prediction from induction period calorimetric measurements on materials undergoing autocatalytic decomposition, Can. J. Chem., 68 (1990) 2111–2114.